Article:
Gross, A, Palchan, D, Krom, MD et al. (1 more author) (2016) Elemental and isotopic composition of surface soils from key Saharan dust sources. Chemical Geology, 442. pp. 54-61. ISSN 0009-2541

https://doi.org/10.1016/j.chemgeo.2016.09.001

Elemental and isotopic composition of surface soils from key Saharan dust sources

A. Gross a,,1, D. Palchana,2, M.D. Kromb,c, A. Angert a
a The Institute of Earth Sciences, The Hebrew University of Jerusalem, Israel
b Department of Marine Biology, Haifa University, Israel
c School of Earth and Environment, Leeds University, Leeds, UK

Abstract

Saharan dust contains significant amount of P, an important macronutrient to all living organisms, which has been shown to exert large effects on nearby and remote ecosystems located across the dust transport pathways.
The biological effect of Saharan dust depends on the amount and nature of the P speciation of the dust. However, thus far relatively small numbers of samples frompotential source areas (PSA) has been analyzed. Here we report the P speciation (resin-P, HCl-P, Fe-bound-P and organic-P), the δ18OP values, the elemental composition, and the 87Sr/86Sr and 143Nd/144Nd of the fine fraction and bulk soil from 5 important PSAs across Northern Africa. We found the HCl-P concentrations between different source areas were relatively constrained but that these concentrations were higher in the fine fraction, which here is used a surrogate for dust. The δ18OP values for soils fromsand dunes varied from15.0 to 21.4‰,which is in the range of phosphate minerals fromsedimentary origin.
The δ18OP values of soils from dry lakes were significantly higher (24.0–28.5‰), probably since their P is derived from fossilized plankton that lived in the lake as it dried up. The 87Sr/86Sr and εNd values ranged from 0.7219 to 7276 and−12.7 to−14.0 in eastern samples and from 0.7146 to 0.7185 and−11.9 to−13.4 inwestern samples, suggesting a different source for the siliciclastic material of eastern and western samples. Our analysis indicates that the δ18OP values are decoupled from the Sr and Nd isotopic systems. Together, the new chemical and isotope data are specific for different PSAs and thus are used for source apportionment purposes. Such data can be used to provide more accurate estimates of the flux of potentially bioavailable P to marine and terrestrial ecosystems. These estimates can be used in global climatemodels to determine themagnitude and distribution of P control on carbon uptake.

Introduction

The Saharan desert is the largest dust source on earth and contributes more than 50% of the global mineral dust load (Goudie and Middleton, 2001; Schutz et al., 1981). Once lifted from the Saharan soils, the dust can spread southward to the Sahel and central Western Africa, northward across the Mediterranean towards Europe (Thevenon et al., 2010), eastward towards the Middle East (Ganor, 1991; Israelevich et al., 2003) and westward across the Atlantic Ocean reaching as far as the Amazon Basin (Prospero et al., 1981; Swap et al.,1992). Because of the large spread of Saharan dust its transport pathways, active sources and chemical composition have been intensively studied ((Scheuvens et al., 2013) and references within).
The Saharan desert covers a large area, and as a result it cannot be referred to as a uniformdust source.Within the Sahara desert, several potential source areas (PSA) have been identified which emit most of the dust burden ((Scheuvens et al., 2013) and references within). Many of these active sources are shown in Fig. 1 (adapted with permission from Scheuvens et al. (2013)) and include Northern Algeria and the “Zone of Chotts” in Tunisia (PSA 1, green), the foothills of the Atlas mountains andWesternMauritania (PSA 2, light blue), Southern Algeria and Northern Mali, near the Ahaggar massif (PSA 3, dark blue), Central Libya (PSA 4, purple), the Bodèlè depression in Western Chad (PSA 5, brown) and Central Egypt and Northern Sudan (PSA 6, red). It has been suggested that the most active sources within these large areas are associated with depressions and dry lakes (Ashpole and Washington, 2013; Prospero et al., 2002). However recent studies revealed

the active dust sources are more diverse and include alluvial fans, dry wadis, sand dunes and anthropogenic surfaces (Bullard et al., 2011; Crouvi et al., 2012; Ginoux et al., 2012; Schepanski et al., 2013; Schepanski et al., 2009).

The most important source of atmospheric P is desert dust, which has been estimated to account for 83% (1.15 Tg P a−1) of the total global source of atmospheric phosphorus (Mahowald et al., 2008). In particular Saharan dust is considered one of the major external suppliers of phosphorus (P) to the Atlantic Ocean (Mills et al., 2004; Okin et al., 2011), to the Mediterranean Sea (Krom et al., 2004) and to America's tropical forests (Gross et al., 2015b; Okin et al., 2004; Swap et al., 1992). The total amount of P in atmospheric dust and its potential bioavailability depends on P mineralogy in the source soils and the subsequent atmospheric processes, which occur during transit to final deposition in the ocean or on land (Nenes et al., 2011; Stockdale, Submitted (PNAS)). Bioavailable P in the ocean is the phase which rapidly dissolves in surface seawater before the refractory minerals drop out of the photic zone. Here this was determined as the P fraction that is extracted by anion exchange resin (resin P phase (Gross et al., 2015a, 2013; Qian and Schoenau, 2002)). In addition, during atmospheric transport, acidic processes in the atmosphere dissolve some fraction of the less bioavailable P fractions such as P that is bound to calcium minerals as apatite or P that is bound to iron minerals (Stockdale,Submitted (PNAS)). Thus, the P phase that is released by 1MHCl extraction represents the potentially bioavailable P in the ocean. On land, the resin P fraction is considered immediately bioavailable to organisms (Cooperband et al., 1999) while the HCl P fraction is likely to become available in longer time scales and thus represents the potentially bioavailable P. At present, the degree of bioavailability of organic P to marine or terrestrial ecosystems is still unknown.

Yang et al. (2013), developed a global estimate of P in source soils based mainly on the soil map of Dürr et al. (2005) and estimates of the effect of desert weathering on the rocks, derived from data obtained in the deserts of SW USA. However, North African dust sources are still poorly characterized. In order to characterize the P speciation of dust that derives from the various PSAs in the Sahara and to predict its biogeochemical effect on nearby or remote ecosystems, data on the P mineralogy of the soils in the source area is required.

Furthermore measurement of relevant different isotopic systems and elemental content of the soils in the source area ca be used to characterize the area within the Sahara desert that is the source of a given sample of dust.

Our aim in this study was to create a data set that includes isotopic values and bulk concentrations of major and trace elements in a serie of soils sampled fromthemajor dust source areas (PSAs) in North Africa.

Our measurements include the isotopic composition of oxygen in phosphate (δ18OP),which can be used to trace Saharan dust-P sources (Grosset al., 2015a, b) and the isotopic ratios of Sr and Nd which have been widely used as fingerprints for particle sources (e.g. Box et al., 2011; Grousset and Biscaye, 2005; Grousset et al., 1992). Our elemental analysis is focused on phosphorus (P) because Saharan dust has been shown to be enriched in P (Gross et al., 2015a, b; Scheuvens et al., 2013) which is crucial for the productivity and carbon uptake of marine and terrestrial ecosystems located across the dust transport pathway (Carbo et al., 2005; Mills et al., 2004; Okin et al., 2004; Swap et al., 1992). Since dust is derived primarily from the soil finest particles, we also examined the elemental and isotopic composition in fine particles (PM10 and PM20) separated from a selected number of soils, as a surrogate for mineral dust (Lafon et al., 2006; Shi et al.,2011b). Overall, the data set presented in this study partly complements older studies and can be used in future studies to identify the source of the Saharan dust, and by characterizing its P speciation, to predict the flux of potentially bioavailable P to globally important marine and terrestrial ecosystems.

2. Methods

2.1. Soil sampling

Table 1 and Fig. 1 details the locations of 13 soil samples used in this study. The soils were collected from the upper soil profile (0–10 cm deep). Samples were ground and sieved to 2 mm and roots, stones, and large fauna were removed by hand. We analyzed 9 bulk samples (TL, IR, LIB1, LIB2, CHT, BODU, JB, EM and AGF (Table 1), 2 (PM10 samples(particles b10 μm, BM and MAL) and 2 PM20 samples (WS and BODI). The fine grain size samples were received from the University of Leeds. For the bulk samples JB, EM, and AGF, particle size separation was generated following the dust tower separation and filtration methods reported by Shi et al. (2011b) and particles b10 μm (PM10) were collected and analyzed (JB, EM, AGF). The fractionated Saharan soils have been shown to be close surrogates to atmospherically sampled dust (Desboeufs et al., 2014; Guieu et al., 2010; Lafon et al., 2006; Shi et al., 2011a). From each soils sample, the first subsample was taken for phosphate oxygen isotopes analysis (δ18OP) and resin P and HCl P determinations. In 8 out of the total 13 samples used in this study (JB, TL, EM, IR, AGF, LIB, BODI, BODU) we had sufficient material for full elemental analysis and Sr and Nd isotopes measurements.

2.2. Soil P determinations

Resin P and HCl P concentrationswere determined for all of our samples (Table 2). The resin P fraction is considered to be indicative of the phosphate pool that is available for plant uptake (Cooperband et al., 1999; Qian and Schoenau, 2002)). The HCl P fractionis considered to be a good approximation of phosphate present in acid soluble P minerals such as apatite and Fe-bound P. To determine the resin P fraction, a subsample of 0.5 g was shaken on an orbital shaker with anion exchange resin membranes (BDH-55164) in 50 ml of double deionized water for 24 h. To elute P from the membranes, the resin membranes were shaken overnight in 5 ml of 0.2 M HNO3 (Gross and Angert, 2015; Weiner et al., 2011). To determine the HCl P, phosphate was extracted from 0.5 g of soil by 50 ml of 1 M HCl for 24 h. Because of the sizes of the sampleswere limited,we didn't have enough material to analyse the Fe-bound P and the organic P fractions in all of our samples. Thus, the Fe-P and organic P were analyzed only for samples JB, EM, LIB1, BM. This analysis was performed following the SPExMan SEDEX sequential extraction scheme presented by Ruttenberg et al. (2009). P concentrations in the extracted solutions were determined by molybdate colorimetry (Murphy and Riley, 1962). The average difference between duplicate samples was 1.3%. The Fe-bound P and the organic P fraction for sample WS reported here, were taken from Nenes et al. (2011).

2.3. ICP-MS elemental analysis

Eight soil samples (JB, TL, EM, IR, AGF, LIB1, BODI and BODU, Table S1) were analyzed for total elemental content of their carbonate and siliciclastic fractions. The carbonate leachate and the siliciclastic fractions were extracted following the method from Palchan et al. (2013).
Twenty-seven elements (Al, Fe, Ca, Mg, Mn, Na, K, Rb, Ba, Th, U, La, Ce, Pb, Pr, Sr, Nd, Sm, Eu, Gd, Tb, Dy, Ho, Er, Tm, Yb, Lu) were analyzed by ICP-MS system (Agilent 7500cx). Rare earth elements (REE) were normalized to Post Archean Australian Shale (PAAS). Prior to the analysis, the ICP-MS was calibrated with a series of ICP multi-element standard solutions VI–Merck Millipore (with concentrations ranging from 1 ppt—100 ng/ml)) and standards of major metals (with concentrations ranging from 300 ng/ml—3 μg/ml). Internal standards (50 ng/ml Sc, 5 ng/ml Re and Rh) were added to every standard and sample for drift correction. We present some of the major element results using the Chemical Index of Alteration (CIA) which is the molecular ratio of the oxides of Al, Ca, Na and K using the formula of (Nesbitt and Young, 1982):
CIA ¼ Al2O3
Al2O3 þ CaO þ Na2O þ K2O
CIA estimates the proportions of the primary and secondary minerals hence is a good measure for the weathering of the samples (Nesbitt and Markovics, 1997), although it should be used cautiously (Li and Yang, 2010).

2.4. δ18OP determinations
Since most of the P in the samples analyzed in this study is bound to HCl extractable minerals (Table 2) we determined the δ18OP values for the HCl P fraction. We followed the method of Tamburini et al. (2010), which is based on extraction of the total inorganic P from the soils with 1 M HCl. The extracted phosphate was precipitated as silver phosphate. For isotopic composition determinations, three replicates of ~0.3 mgsilver phosphatewere packed in silver capsules and introduced into a high temperature pyrolysis unit (HT-EA), where they were converted to CO in the presence of glassy carbon tube placed inside the unit reactor (Vennemann et al., 2002). The HT-EA is interfaced in continuous-flowmode, through a gas chromatograph column, to an isotope ratio mass spectrometer (Sercon 20-20). All isotopic values are given in the delta-notation versus VSMOW (Vienna Standard Mean Ocean Water). The average standard deviation between three replicates of the same sample was 0.3‰. All measurements were performed against Ag3PO4 laboratory standards, which were calibrated against the following Ag3PO4 standards, with their (isotopic signatures in parentheses): TU-1 (21.1‰) and TU-2 (5.4‰; (Vennemann et al., 2002), UMCS-1

(32.6‰) andUMCS-2 (19.4‰; (Halas et al., 2011) and against IAEA-601 benzoic acid standard (23.3‰; (Coplen et al., 2006)). 2.5. Sr and Nd isotopic ratio determinations In order to elute and separate the Sr and Nd fromthe soils, solutions of eight soil samples were passed through resins following the procedure of Palchan et al. (2013). Isotopic analysis was carried out using
Neptune multi collector mass spectrometer. SRM 987 standard was run every 10 samples for Sr with average value of 87Sr/86Sr = 0.71024 ± 6 (2σ, n = 10). JNdi standard was run every 10 samples for Nd with average value of 143Nd/144Nd= 0.51208 ± 4 (2σ,n = 20).
The Nd isotopic values are expressed as εNd=[[143Nd/144Nd](meas.) /[143Nd/144Nd](CHUR)-1] × 104, where CHUR = 0.512638 (JacobsenandWasserburg, 1980).

2.6. Statistical analysis
Comparisons between the soils were made using post-hoc Tukey HSD analysis and significant differences were determined at p b 0.05.

3. Results
3.1. P concentrations
The majority of the P in all samples was inorganic and extracted by HCl while the Fe-bound P and the organic P amounts were generally low (Table 2). TheHCl P concentrations in the bulk sampleswere similar within the same PSA and between PSA1, PSA2, PSA3 and PSA5 (Table 2) and ranged from 440 to 570 μg P g−1 soil. However, significantly higher HCl P concentration (p b 0.05) in the bulk samples were found in PSA4 (760 and 700 μg P g−1 soil for LIB1 and LIB2, respectively).
In the samples that were analyzed for both the bulk and PM10 fractions the HCl P concentrations, resin P concentrations and P solubility were significantly higher in the fine fraction (p b 0.05, Table 2) than the bulk. The HCl P concentrations, resin P concentrations and P solubility were significantly higher in the PM10 than in the bulk for JB, EM and AGF. (p b 0.05, Table 2).

3.2. Elemental composition
The concentration of major and trace elements in the carbonate leachate and the siliciclastic fractions termed L1 and L2, respectively, are given in Table S1. The CIA values of the L2 range from 65 to 85 where higher values correlate with lower latitudes (excluding the LIB1 sample (Fig. 2)). Al and Fe oxides content of the L2 fraction vary from 1 wt% to 18 wt% and 0.3 wt% to 7.5 wt%, respectively. The L1 fraction shows practically zero wt.% of these metal oxides indicating there was considerable enrichment in the L2 fraction (Fig. 3). The enrichment of these metals is an indication for the leaching of soluble elements from the sample (e.g. Haliva-Cohen et al., 2012). Ca andMg oxides of the entire data set ranged from 0.1 wt% to 10 wt%. The L1 fraction showed a strong correlation between Mg and Ca but this correlation did not show in the L2 fraction (Fig. 4). REE patterns from the various regions showed considerable changes between the PSAs (p b 0.05).

Samples from PSA5 and PSA3 had a unique signature with a weak Eu anomaly whereas samples from PSA2 clearly show this anomaly (Fig. S1).

3.3. δ18OP values

The δ18OP values varied significantly between soils (Table 2, p b 0.05) and ranged from 15.0 ± 0.2‰ (TL) to 28.5 ± 0.2‰ (BODU). The δ18OP values in soils from Morocco, at the Northern edge of PSA2 (JB, IR, EM, Fig. 1) fell in a narrow range (17.1 ± 0.3‰ to 17.3 ± 0.3‰) except in TL that had significantly lower values (15.0±0.2‰). These values overlapped with the values of LIB1 (PSA4) from Northern Libya (17.0 ± 0.6‰). The δ18OP values of WS (PSA2), LIB2 (PSA4) and CHT (PSA1) were significantly higher (19.6 ± 0.4‰, 21.6 ± 0.1‰ and 20.8 ± 0.1‰, respectively, p b 0.05). The highest δ18OP values were found in samples taken from dry lake beds, AGF (24.0 ± 0.3‰), BODI (25.5 ± 0.2‰) and BODU (28.5 ± 0.2‰). Particle size separation treatments did not alter or altered only slightly the δ18OP values (Table 2).

3.4. Sr and Nd isotopes

Sr and Nd isotopic ratios of the insoluble residue of the soil samples were plotted on a Sr\\Nd diagram (Fig. 5). The 87Sr/86Sr values ranged from 0.71467 to 0.72764 and the εNd ranged from −14 to −11.9 except for the southernmost sample (AGF), which is characterized by 87Sr/86Sr value of 0.75402 and εNd value of −17.2 (Table 3).

4. Discussion

4.1. Elemental characterization

The geochemical analysis showed local and regional variability between Saharan soils and dust from different source regions (Table S1), in accordance with numerous previous studies that report the elemental composition of Saharan dust depends on the source region (Caquineau et al., 2002, 1998; Formenti et al., 2008; Scheuvens et al.,2013). The concentrations of Fe and K, which are also important nutrients tomany organisms in the terrestrial and marine ecosystems, varied not only between PSA1-5 but also within the same PSA. This suggests that local environmental changes possibly related to lithological and weathering changes (Shi et al., 2011b) can alter the Fe and K content and biological availability in dust and thus its biogeochemical effect.

This local variability indicates that it will be hard to predict the nutrient (Fe and K) concentration in dust based simply on its source location and hence it's biogeochemical effect. The samples showed dependence of the CIA upon latitude interpreted as due to increased rainfall towards subtropical latitudes (Fig. 2). Samples from PSA2, which is the location upwind from marine corps sampled off Western Africa show lower CIA values than those reported for siliciclastic dust in these cores (Cole et al., 2009). The former weathering trend is not seen in the Fe oxide similarly to the observations of Scheuvens et al. (2013). Nonetheless, we found that the content of Fe and Al oxides can serve as a tool to discriminate between the various PSAs (Fig. 3). The content of Ca and Mg oxides in the L1 fraction shows a good correlation due to the strong association of carbonate minerals calcite and dolomite (Fig. 4). The L2 fraction content of Mg oxide probably reflects the presence of palygorskite which is a common magnesium bearing clay mineral that occurs in arid environments (Singer, 1984). We have showed that based on the REE content we can differentiate the sources from PSA2 and the other PSA5 and PSA4 due to the different patterns of the Eu anomaly (Fig. S1, p b 0.05). The REE patterns of soils from PSA4 were similar to the pattern found in sediments fromthe Red Sea that were deposited during the Pleistocene (Palchan et al., 2013), indicating the origin of these particular sediments is likely fromPSA4 in northern Sahara.

4.1.1. P concentrations

In contrast to the variability in the elemental composition of the other major and rare earth elements, the variability in the P concentrations for soils within the same PSA and between PSA's was much more constrained. The bulk of the P in Saharan soils is attached to calcium minerals such

as apatites, which is the HCl-P minus Fe-Bound-P as defined within the SEDEX fractionation scheme ((Ruttenberg, 1992), Table 2). The similarity in P concentration may be an indication to a relatively homogenous distribution of detrital apatite's in most of the desert soils. The significantly higher HCl P concentrations found in PSA 4 may be an indication that these soils are lying adjacent to a sedimentary phosphorite deposit which are common in the Saharan desert. The significantly higher P concentrations in PSA 4 shows that some dust source area are enriched in P in relative to others. This suggests that the identification of the source area of a specific dust storm is important to predict the amount of potentially bioavailable P concentrations in a given sample of Saharan dust. These results are in line with previous analysis of P in Saharan dust that report that dust P concentration vary significantly between dust events, owing to differences in P concentrations in the areas identified by remote sensing as the sources of individual dust events (Gross et al., 2015a). Thus, our evidence from this and EMand IR) suggests their siliciclastic material is either derived from different sources or that their siliciclastic material is derived from a uniform source but the Sr and Nd isotopic values were affected by the grain size differences in the bulk., However, overall the Sr and Nd values in Western Sahara are significantly different than that in soils from Eastern Sahara. Similar values to the Sr and Nd values we report for PSA2 (within error margins) are found off shore from western Africa in core ODP 658C (Cole et al., 2009; Grousset et al., 1988, 1998). The Nd\\Sr isotopic system does not always provide clear identification of the source area and the isotopic values may overlap between different PSAs such as in samples from Libya and Chad. Yet, the phosphate δ18OP values differed markedly between these two areas (because of the difference in the phosphate origin), suggesting that the combination of Sr and phosphate oxygen isotopic systems can be used for source identification in these cases (Fig. 6).

5. Summary

In summary the amount of bioavailable P supplied to marine and terrestrial ecosystems via Saharan dust depends on the nature and concentration of P in the source area aswell as on subsequent acid processes in the atmosphere (Nenes et al., 2011; Stockdale, Submitted (PNAS)).

Our analysis of 87Sr/86Sr and 144Nd/143Nd extends the existing data set of Sr and Nd isotopic systems in various Saharan soils, sediments and dust samples (Scheuvens et al., 2013) though still only represents a limited fraction of the total area of the Sahara desert. We provide the first data set of phosphate δ18OP values in Saharan soil samples. Our analysis of this unique isotopic system shows that the soil's P origin is regionally different for different PSAs and is decoupled from the 87Sr/86Sr and 144Nd/143Nd isotopic systems. Thus, we suggest that in cases where the isotopic values of the phosphate minerals are similar, combining the δ18OP values with other isotopic systems such as Sr and Nd can be useful in identifying the source location of the dust. This shows that a multi-proxy approach including also elemental and mineralogical data will sometimes be necessary to assign a dust sample to a specific potential source area.

Our measurements point to a regional trend in the soil P concentrations across the Sahara, in contrast to previous reports (Scheuvens et al., 2013). Existing maps of P content in Saharan soils (E.g.(Yang et al., 2013)) use indirect methods to estimate the amount of P in dust source locations. The data obtained in this study provide direct measurements, which enables the source location of sampled dust to be identified. It also offers the potential of a more sophisticated estimate of the potentially bioavailable P being supplied from different regions (PSAs) of the Saharan desert. Such values combined with back trajectory data, when incorporated into global climate models, will enable more accurate estimates of the effect of P delivered from Saharan sources on the carbon dioxide uptake rates in both offshore oceanic systems and terrestrial systems such as the Amazon forest.

Acknowledgments

This researchwas supported by a Grant fromthe Israel Science Foundation (#45/14) and a grant from the GIF, the German-Israeli Foundation for Scientific Research (#1139/2011). A.G. was funded by the

Israel Ministry of Science and Technology (MOST). MDK was funded by a grant from the Leverhulme Trust entitled “understanding the delivery of phosphorus nutrient to the oceans” Grant Number RPG 406. We thank Jim McQuaid and Zongbo Shi from the University of Leeds and University of Birmingham respectively for sharing their soil samples with us.

Appendix A. Supplementary data

Supplementary data to this article can be found online at http://dx.doi.org/10.1016/j.chemgeo.2016.09.001.

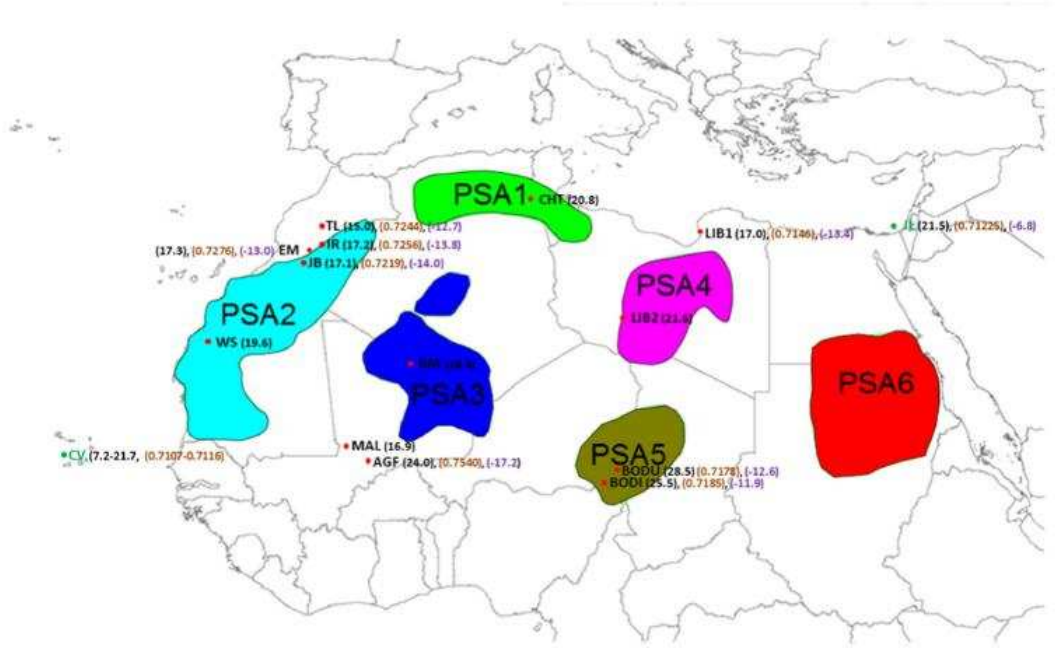

Fig. 1. Map of North Africa (adapted with permission from Scheuvens et al. (2013)) showing potential source areas (PSA1 to 6, different colors), locations of soil and dust sampling sites (red and green dots, respectively) and the spatial distribution of $\delta^{18}O_p$ values (black), $^{87}Sr/^{86}Sr$ values (brown) and εNd(0) values (gray). The isotopic values for the dust samples were taken from Gross et al. (2015a) and Palchan et al. (2013). (For interpretation of the references to colour in this figure legend, the reader is referred to the web version of this article.)

Table 1
The soils used in this study. Sample list including location, coordinates, class and particle size.

Sample name (code)	PSA	Location	Coordinates	Class	Particle size
Chott el Djerid (CHT)	1	Tunisia	33°39°N, 8°18°E	Sahara, drainage basin	Bulk
Jebel Brahim (JB)	2	Morocco	29°56°N, 5°37°W	Sahara, sand dune	Bulk + PM 10
Trab Labied (TL)	2	Morocco	31°17°N, 6°57°W	Sahara, sand dunes	Bulk
El Miyit (EM)	2	Morocco	30°21°N, 5°37°W	Sahara, sand dunes	Bulk + PM 10
Iriki (IR)	2	Morocco	29°59°N, 6°35°W	Sahara, sand dunes	Bulk
W-Sahara (WS)	2	Western Sahara	24°24°N, 12°07°W	Sahara, sand dunes	PM 20
Bordj Mokhtar (BM)	3	Algeria	21°19°N, 0°56°E	Sahara, sand dunes	PM 10
Lake Agoufou (AGF)	3	Mali	15°10°N, 0°38°E	Sahel, dry lake	Bulk + PM 20
Libya 1 (LIB1)	4	Libya	32°50°N, 22°21°E	Sahara, sand dunes	Bulk
Libya 2 (LIB2)	4	Libya	26°34°N, 12°34°E	Sahara, Sand dunes	Bulk
Bodélé lakebed (BODI)	5	Chad	16°41°N, 17°47°E	Sahara, dry lake	PM 20
Bodélé dune (BODU)	5	Chad	16°52°N, 18°52°E	Sahara, dry lake + sand dunes	Bulk

Table 2
P concentrations using different chemical extraction methods (in μg P g soil^{-1}) and HCl P $\delta^{18}O_p$ values and P solubility of bulk soil samples and PM_{10} or PM_{20} size fractions (in brackets). [a]Analytical standard error of <1%. [b]Taken from Nenes et al. (2011) and Shi et al. (2011b). N/D = not determined.

Country	Tunisia	Morocco	Morocco	Morocco	Morocco	Morocco	Morocco	W. Sahara	Algeria	Mali	Mali	Mali	Libya	Libya	Chad	Chad
Class	CHT	JB	JB	TL	EM	EM	IR	WS	BM	MAL	AGF	AGF	LIB1	LIB2	BODI	BODU
PSA	1	2	2	2	2	2	2	2	3	3	3	3	4	4	5	5
Size Fraction	Bulk	Bulk	PM_{10}	Bulk	Bulk	PM_{10}	Bulk	PM_{20}	PM_{10}	PM_{10}	Bulk	PM_{10}	Bulk	Bulk	PM_{20}	Bulk
$\delta^{18}O_P$ (‰)	20.8 ± 0.1	17.1 ± 0.1	17.5 ± 0.4	15.0 ± 0.2	17.3 ± 0.3	17.6 ± 0.4	17.2 ± 0.3	19.6 ± 0.4	18.4 ± 0.2	16.9 ± 0.5	24.0 ± 0.3	23.4 ± 0.5	17.0 ± 0.6	21.6 ± 0.1	25.5 ± 0.2	28.5 ± 0.2
Resin-P (μg g^{-1} soil)[a]	N/D	4	70	3	7	95	3	40	110	75	15	20	10	15	10	15
Ca-P (μg g^{-1} soil)[a]	570	440	620	470	480	780	570	660	780	720	440	550	760	700	450	510
Fe-P (μg g^{-1} soil)[b]	N/D	9	N/D	N/D	7	N/D	N/D	78	16	N/D	N/D	N/D	16	N/D	N/D	N/D
Organic-P (μg g−1 soil)[b]	N/D	30	N/D	N/D	32	N/D	N/D	87	80	N/D	N/D	N/D	172	N/D	N/D	N/D
P solubility (%)[a]	N/D	1	15	0.5	1.5	13	0.5	7	15	10	3	4	1	2	2	3

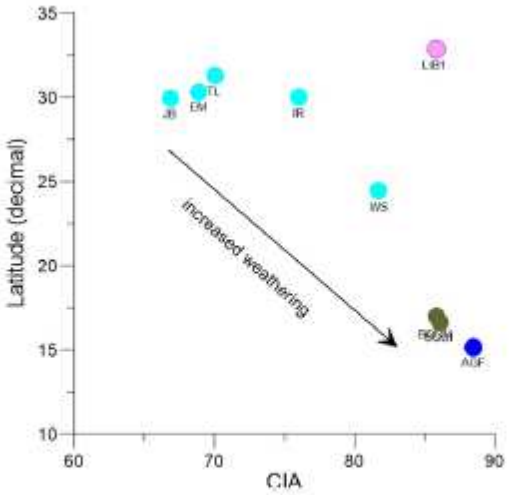

Fig. 2. Depiction of the chemical index of alteration (CIA; see text). All samples indicate the siliciclastic fraction with coloring following Fig. 1.

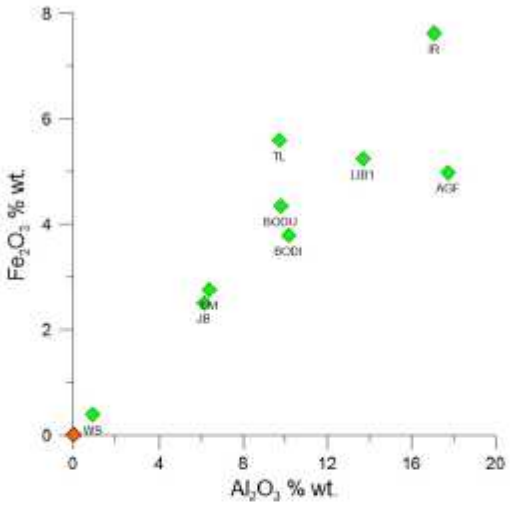

Fig. 3. Log based diagram of CaO versus MgO in % wt. Carbonate fraction is indicated in orange and siliciclastic fraction is indicated with green. (For interpretation of the references to colour in this figure legend, the reader is referred to the web version of this article.)

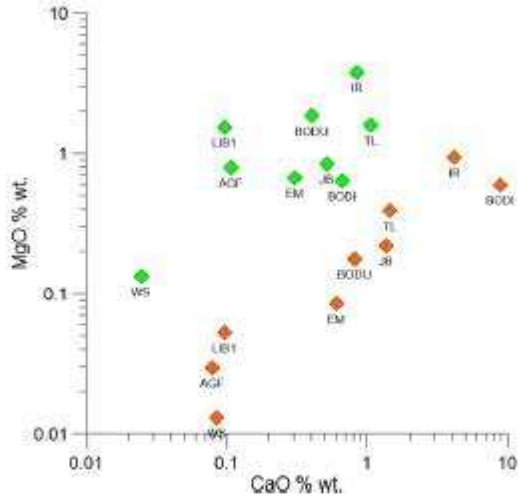

Fig. 4. Al_2O_3 versus Fe_2O_3 of the carbonate fraction (orange) and for the siliciclastic fraction (green). (For interpretation of the references to colour in this figure legend, the reader is referred to the web version of this article.)

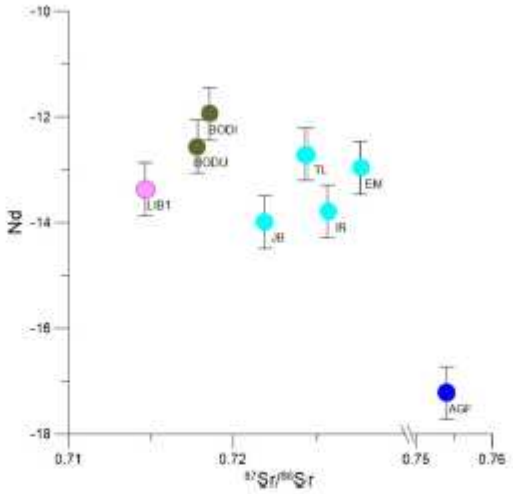

Fig. 5. $^{87}Sr/^{86}Sr$ versus εNd (0) for soil samples from PSA2 (light blue) PSA3 (dark blue), PSA4 (pink) and PSA5 (beige). (For interpretation of the references to colour in this figure legend, the reader is referred to the web version of this article.)

Table 3
Rb, Sr, Sm, and Nd concentrations and Sr and Nd isotope data of the of the siliciclastic fraction of bulk soils (for samples JB, TL, EM, IR, AGF, LIB1 and BODU) and PM_{20} fraction (BODI).

Country	Morocco	Morocco	Morocco	Morocco	Mali	Libya	Chad	Chad
Class	JB ^{Bulk}	TL ^{Bulk}	EM ^{Bulk}	IR ^{Bulk}	AGF ^{Bulk}	LIB1 ^{Bulk}	BODI ^{PM20}	BODU ^{Bulk}
PSA	2	2	2	2	3	4	5	5
Rb (ppm)[a]	51.0	79.1	56.6	135.4	124.1	57.2	53.3	67.1
Sr (ppm)[a]	65.0	79.3	56.4	110.5	55.9	202.8	76.4	75.5
Rb/Sr	0.784	0.997	1.004	1.225	2.221	0.282	0.698	0.888
$^{87}Sr/^{86}Sr$	0.72194	0.72441	0.72764	0.72565	0.75402	0.71467	0.71858	0.71785
2σ	7. E−05	3. E−05	4.E−05	2.E−05	2.E−05	2.E−05	2.E−05	2.E−05
Nd (ppm)[a]	14.4	26.5	16.9	34.4	46.6	33.2	32.7	25.9
Sm (ppm)[a]	2.6	4.9	3.0	6.5	8.6	6.2	5.9	4.6
Sm/Nd	0.1789	0.1837	0.1765	0.1888	0.1834	0.1860	0.1799	0.1777
$^{143}Nd/^{144}Nd$	0.511921	0.511987	0.511973	0.511931	0.511755	0.511953	0.512026	0.511994
εNd (0)	−14.0	−12.7	−13.0	−13.8	−17.2	−13.4	−11.9	−12.6
2σ	9. E−06	8.E−06	8.E−06	8.E−06	1.−E−05	1. E−05	8.E−06	9.E−06

[a] Analytical standard error of <5–10%.

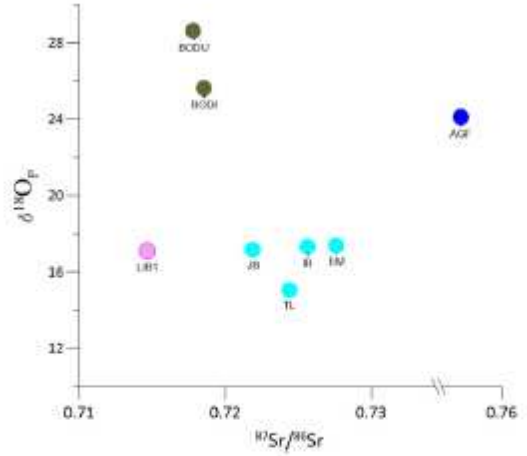

Fig. 6. $^{87}Sr/^{86}Sr$ versus $\delta^{18}O_P$ values for soil samples from PSA2 (light blue) PSA3 (dark blue), PSA4 (pink) and PSA5 (beige). (For interpretation of the references to colour in this figure legend, the reader is referred to the web version of this article.)

References

Anderson, L.D., Faul, K.L., Paytan, A., 2010. Phosphorus associations in aerosols: what can they tell us about P bioavailability? Mar. Chem. 120 (1–4), 44–56.

Angert, A., Weiner, T., Mazeh, S., Sternberg, M., 2012. Soil phosphate stable oxygen isotopes across rainfall and bedrock gradients. Environ. Sci. Technol. 46 (4), 2156–2162.

Ashpole, I., Washington, R., 2013. A new high-resolution central and western Saharan summer time dust source map from automated satellite dust plume tracking. J. Geophys. Res. Atmos. n/a-n/a.

Box, M.R., et al., 2011. Response of the Nile and its catchment to millennial-scale climatic change since the LGM from Sr isotopes and major elements of East Mediterranean sediments. Quat. Sci. Rev. 30 (3–4), 431–442.

Bristow, C.S., Hudson-Edwards, K.A., Chappell, A., 2010. Fertilizing the Amazon and equatorial Atlantic with West African dust. Geophys. Res. Lett. 37.

Bullard, J.E., et al., 2011. Preferential dust sources: A geomorphological classification designed for use in global dust-cycle models. J. Geophys. Res. Earth Surf. 116.

Caquineau, S., Gaudichet, A., Gomes, L., Legrand, M., 2002. Mineralogy of Saharan dust transported over northwestern tropical Atlantic Ocean in relation to source regions. J. Geophys. Res. Atmos. 107 (D15) AAC 4-1-AAC 4-12.

Caquineau, S., Gaudichet, A., Gomes, L., Magonthier, M.-C., Chatenet, B., 1998. Saharan dust: clay ratio as a relevant tracer to assess the origin of soil-derived aerosols. Geophys. Res. Lett. 25 (7), 983–986.

Carbo, P., Krom, M.D., Homoky,W.B., Benning, L.G., Herut, B., 2005. Impact of atmospheric deposition on N and P geochemistry in the southeastern Levantine basin. Deep-Sea Res. II Top. Stud. Oceanogr. 52 (22−23), 3041–3053.

Cole, J.M., et al., 2009. Contrasting compositions of Saharan dust in the eastern Atlantic Ocean during the last deglaciation and African humid period. Earth Planet. Sci. Lett. 278, 257–266.

Cooperband, L.R., Gale, P.M., Comerford, N.B., 1999. Refinement of the anion exchange membrane method for soluble phosphorus measurement. Soil Sci. Soc. Am. J. 63 (1), 58–64.

Coplen, T.B., et al., 2006. New guidelines for delta C-13 measurements. Anal. Chem. 78 (7), 2439–2441.

Crouvi, O., Schepanski, K., Amit, R., Gillespie, A.R., Enzel, Y., 2012. Multiple dust sources in the Sahara Desert: the importance of sand dunes. Geophys. Res. Lett. 39.

Desboeufs, K., Leblond, N.,Wagener, T., Bon Nguyen, E., Guieu, C., 2014. Chemical fate and settling of mineral dust in surface seawater after atmospheric deposition observed from dust seeding experiments in large mesocosms. Biogeosciences 11 (19), 5581–5594.

Dürr, H.H., Meybeck, M., Dürr, S.H., 2005. Lithologic composition of the Earth's continental surfaces derived froma newdigitalmap emphasizing riverine material transfer. Glob. Biogeochem. Cycles 19 (4) n/a-n/a.

Formenti, P., et al., 2008. Regional variability of the composition of mineral dust from western Africa: Results from the AMMA SOP0/DABEX and DODO field campaigns. J. Geophys. Res. Atmos. 113 (D23) n/a-n/a.

Ganor, E., 1991. The composition of clay minerals transported to Israel as indicators of Saharan dust emission. Atmos. Environ. Part A 25 (12), 2657–2664.

Gasse, F., 2002. Diatom-inferred salinity and carbonate oxygen isotopes in Holocene waterbodies of thewestern Sahara and Sahel (Africa). Quat. Sci. Rev. 21 (7), 737–767.

Ginoux, P., Prospero, J.M., Gill, T.E., Hsu, N.C., Zhao, M., 2012. Global-scale attribution of anthropogenic and natural dust sources and their emission rates based on Modis deep blue aerosol products. Rev. Geophys. 50.

Goudie, A.S., Middleton, N.J., 2001. Saharan dust storms: nature and consequences. Earth Sci. Rev. 56 (1–4), 179–204.

Gross, A., Angert, A., 2015. What processes control the oxygen isotopes of soil bio-avail

Gross, A., Turner, B.L., Goren, T., Berry, A., Angert, A., 2015b. Tracing the sources of atmospheric phosphorus deposition to a tropical rain Forest in Panama using stable oxygen isotopes. Environ. Sci. Technol.

Gross, A., Nishri, A., Angert, A., 2013. Use of phosphate oxygen isotopes for identifying atmospheric-p sources: a case study at lake kinneret. Environ. Sci. Technol. 19 (47(6)), 2721–2727.

Gross, A., et al., 2015a. Variability in Sources and Concentrations of Saharan Dust Phosphorus Over the Atlantic Ocean Environmental Science & Technology Letters.

Grousset, F., Biscaye, P., Zindler, A., Prospero, J., Chester, R., 1988. Neodymium isotopes as tracers in marine sediments and aerosols: North Atlantic. Earth Planet. Sci. Lett. 87 (4), 367–378.
Grousset, F., et al., 1998. Saharan wind regimes traced by the Sr–Nd isotopic composition of subtropical Atlantic sediments: last glacial maximum vs today. Quat. Sci. Rev. 17 (4), 395–409.
Grousset, F.E., Biscaye, P.E., 2005. Tracing dust sources and transport patterns using Sr, Nd and Pb isotopes. Chem. Geol. 222 (3–4), 149–167.
Grousset, F.E., Rognon, P., Coudegaussen, G., Pedemay, P., 1992. Origins of Peri-Saharan dust deposits traced by their Nd and Sr isotopic composition. Palaeogeogr. Palaeoclimatol. Palaeoecol. 93 (3–4), 203–212.
Guieu, C., et al., 2010. Large clean mesocosms and simulated dust deposition: a new methodology to investigate responses of marine oligotrophic ecosystems to atmospheric inputs. Biogeosciences 7 (9), 2765–2784.
Halas, S., Skrzypek, G., Meier-Augenstein, W., Pelc, A., Kemp, H.F., 2011. Inter-laboratory calibration of new silver orthophosphate comparison materials for the stable oxygen isotope analysis of phosphates. Rapid Commun. Mass Spectrom. 25 (5), 579–584.
Haliva-Cohen, A., Stein, M., Goldstein, S.L., Sandler, A., Starinsky, A., 2012. Sources and transport routes of fine detritus material to the late quaternary Dead Sea basin. Quat. Sci. Rev. 50, 55–70.
Hudson-Edwards, K.A., Bristow, C.S., Cibin, G., Mason, G., Peacock, C.L., 2014. Solid-phase phosphorus speciation in Saharan Bodélé depression dusts and source sediments. Chem. Geol. 384, 16–26.
Israelevich, P.L., Ganor, E., Levin, Z., Joseph, J.H., 2003. Annual variations of physical properties of desert dust over Israel. J. Geophys. Res.-Atmos. 108 (D13).
Jacobsen, S.B.,Wasserburg, G.J., 1980. Sm-Nd isotopic evolution of chondrites. Earth Planet. Sci. Lett. 50 (1), 139–155.
Katra, I., et al., 2016. Substantial dust loss of bioavailable phosphorus from agricultural soils. Sci. Rep. 6, 24736.
Knippertz, P., Christoph, M., Speth, P., 2003. Long-term precipitation variability in Morocco and the link to the large-scale circulation in recent and future climates. Meteorog. Atmos. Phys. 83 (1–2), 67–88.
Krom, M., Herut, B., Mantoura, R., 2004. Nutrient budget for the Eastern Mediterranean: Implications for phosphorus limitation. Limnol. Oceanogr. 49 (5), 1582–1592.
Küster, D., Liégeois, J.-P., Matukov, D., Sergeev, S., Lucassen, F., 2008. Zircon geochronology and Sr, Nd, Pb isotope geochemistry of granitoids from Bayuda Desert and Sabaloka (Sudan): evidence for a Bayudian event (920–900 Ma) preceding the pan-African orogenic cycle (860–590 Ma) at the eastern boundary of the Saharan Metacraton. Precambrian Res. 164 (1), 16–39.
Lafon, S., Sokolik, I.N., Rajot, J.L., Caquineau, S., Gaudichet, A., 2006. Characterization of iron oxides in mineral dust aerosols: Implications for light absorption. J. Geophys. Res. Atmos. 111 (D21) n/a-n/a.
Li, C., Yang, S., 2010. Is chemical index of alteration (CIA) a reliable proxy for chemical weathering in global drainage basins? Am. J. Sci. 310 (2), 111–127.
Mahowald, N., et al., 2008. Global distribution of atmospheric phosphorus sources, concentrations and deposition rates, and anthropogenic impacts. Glob. Biogeochem. Cycles 22 (4). http://dx.doi.org/10.1029/2008gb003240.
Mills, M.M., Ridame, C., Davey, M., La Roche, J., Geider, R.J., 2004. Iron and phosphorus colimit nitrogen fixation in the eastern tropical North Atlantic. Nature 429 (6989), 292–294.
Mizota, C., Domon, Y., Yoshida, N., 1992. Oxygen isotope composition of natural phosphates from volcanic ash soils of the Great Rift Valley of Africa and east Java, Indonesia. Geoderma 53 (1–2), 111–123.
Murphy, J., Riley, J.P., 1962. A modified single solution method for the determination of phosphate in natural waters. Anal. Chim. Acta 27, 31–36.
Nenes, A., et al., 2011. Atmospheric acidification of mineral aerosols: a source of bioavailable phosphorus for the oceans. Atmos. Chem. Phys. 11 (13), 6265–6272.
Nesbitt, H., Young, G., 1982. Early Proterozoic climates and plate motions inferred from major element chemistry of lutites. Nature 299 (5885), 715–717.
Nesbitt, W.H., Markovics, G., 1997.Weathering of granodioritic crust, long-termstorage of elements in weathering profiles, and petrogenesis of siliciclastic sediments. Geochim. Cosmochim. Acta 61 (8), 1653–1670.
Okin, G.S., Mahowald, N., Chadwick, O.A., Artaxo, P., 2004. Impact of desert dust on the biogeochemistry of phosphorus in terrestrial ecosystems. Glob. Biogeochem. Cycles 18 (2). http://dx.doi.org/10.1029/2003GB002145.
Okin, G.S., et al., 2011. Impacts of atmospheric nutrient deposition on marine productivity: roles of nitrogen, phosphorus, and iron. Glob. Biogeochem. Cycles 25.
Palchan, D., Stein, M., Almogi-Labin, A., Erel, Y., Goldstein, S.L., 2013. Dust transport and synoptic conditions over the Sahara–Arabia deserts during the MIS6/5 and 2/1 transitions from grain-size, chemical and isotopic properties of Red Sea cores. Earth Planet. Sci. Lett. 382, 125–139.
Prospero, J.M., Ginoux, P., Torres, O., Nicholson, S.E., Gill, T.E., 2002. Environmental characterization of global sources of atmospheric soil dust identified with the Nimbus 7 Total ozone mapping spectrometer (TOMS) absorbing aerosol product. Rev. Geophys. 40 (1).
Prospero, J.M., Glaccum, R.A., Nees, R.T., 1981. Atmospheric transport of soil dust from Africa to south-America. Nature 289 (5798), 570–572.
Qian, P., Schoenau, J.J., 2002. Practical applications of ion exchange resins in agricultural and environmental soil research. Can. J. Soil Sci. 82 (1), 9–21.
Ruttenberg, K.C., 1992. Development of a sequential extraction method for different forms of phosphorus in marine sediments. Limnol. Oceanogr. 37 (7), 1460–1482.
Ruttenberg, K.C., et al., 2009. Improved, high-throughput approach for phosphorus speciation in natural sediments via the SEDEX sequential extraction method. Limnol. Oceanogr. Methods 7 (5), 319–333.
Schepanski, K., et al., 2009. Meteorological processes forcing Saharan dust emission inferred from MSG-SEVIRI observations of subdaily dust source activation and numerical models. J. Geophys. Res.-Atmos. 114.
Schepanski, K., et al., 2013. Characterization of dust emission from alluvial sources using aircraft observations and high-resolution modeling. J. Geophys. Res.-Atmos. 118 (13), 7237–7259.
Scheuvens, D., Schutz, L., Kandler, K., Ebert, M., Weinbruch, S., 2013. Bulk composition of northern African dust and its source sediments - a compilation. Earth Sci. Rev. 116, 170–194.

Schutz, L., Jaenicke, R., Pietrek, H., 1981. Saharan dust transport over the North Atlantic Ocean. Geol. Soc. Am. Spec. Pap. 186, 87–100.
Shemesh, A., Kolodny, Y., Luz, B., 1983. Oxygen isotope variations in phosphate of biogenic apatites. 2. Phosphorite rocks. Earth Planet. Sci. Lett. 64 (3), 405–416.
Shemesh, A., Kolodny, Y., Luz, B., 1988. Isotope geochemistry of oxygen and carbon in phosphate and carbonate of phosphorite francolite. Geochim. Cosmochim. Acta 52 (11), 2565–2572.
Shi, Z., Bonneville, S., Krom, M.D., Carslaw, K.S., Jickells, T.D., Baker, A.R., Benning, L.G., 2011a. Iron dissolution kinetics of mineral dust at low pH during simulated atmospheric processing. Atmos. Chem. Phys. 11 (3), 995–1007.
Shi, Z., Krom, M.D., Bonneville, S., Baker, A.R., Bristow, C., Drake, N., Mann, G., Carslaw, K., McQuaid, J.B., Jickells, T., 2011b. Influence of chemical weathering and aging of iron oxides on the potential iron solubility of Saharan dust during simulated atmospheric processing. Glob. Biogeochem. Cycles 25 (2).
Singer, A., 1984. Pedogenic Palygorskite in the Arid Environment*. In: Singer, A., Galan, E. (Eds.), Developments in Sedimentology. Elsevier, pp. 169–176.
Stockdale, A., Krom, M.D.,Mortimer, R.J.G., Benning, L.G., Carslaw, K.S., Herbert, R.J., Shi, Z., Mihalopoulos, N., Nenes, A., (PNAS). Supply of bioavailable phosphorus to the oceans: understanding the nature of atmospheric acid processing of mineral dusts. Proc. Natl. Acad. Sci. Submitted for publication
Swap, R., Garstang,M., Greco, S., Talbot, R., Kallberg, P., 1992. Saharan dust in the Amazon Basin. Tellus Ser. B Chem. Phys. Meteorol. 44 (2), 133–149.
Tamburini, F., Bernasconi, S.M., Angert, A.,Weiner, T., Frossard, E., 2010. A method for the analysis of the δ18O of inorganic phosphate in soils extracted with HCl. Eur. J. Soil Sci. 61 (6), 1025–1032.
Tamburini, F., et al., 2012. Oxygen isotopes unravel the role of microorganisms in phosphate cycling in soils. Environ. Sci. Technol. 46 (11), 5956–5962.
Thevenon, F., Chiaradia, M., Adatte, T., Hueglin, C., Poté, J., 2010. Ancient versus modern mineral dust transported to high-altitude alpine glaciers evidences Saharan sources and atmospheric circulation changes. Atmos. Chem. Phys. Discuss. 10 (8), 20167–20191.
Vennemann, T.W., Fricke, H.C., Blake, R.E., O'Neil, J.R., Colman, A., 2002. Oxygen isotope analysis of phosphates: a comparison of techniques for analysis of Ag_3PO_4. Chem. Geol. 185 (3–4), 321–336.
Weiner, T., et al., 2011. A method for analyzing the δ18O of resin-extractable soil inorganic phosphate. Rapid Commun. Mass Spectrom. 25 (5), 624–628.
Yang, X., Post, W.M., Thornton, P.E., Jain, A., 2013. The distribution of soil phosphorus for global biogeochemical modeling. Biogeosciences 10 (4), 2525–2537.
Yu, H., et al., 2015. The fertilizing role of African dust in the Amazon rainforest: A first multiyear assessment based on data fromcloud-aerosol Lidar and infrared pathfinder satellite observations. Geophys. Res. Lett. 42 (6), 1984–1991.